

NUMERICAL SIMULATION OF PRESTRESSED CONCRETE CROSSTIE AND FASTENING SYSTEM

Zhe Chen, Graduate Research Assistant, Dept. of Civil Engineering, University of Illinois at Urbana-Champaign, IL

Moochul Shin, PhD, Postdoctoral Research Associate, Dept. of Civil Engineering, University of Illinois at Urbana-Champaign, IL

Bassem Andrawes, PhD, Assistant Professor, Dept. of Civil Engineering, University of Illinois at Urbana-Champaign, IL

ABSTRACT:

Prestressed concrete crosstie provides a better alternative to traditional wood tie for its improved mechanical characteristics and durability, especially in meeting the performance demand due to increasing freight axle loading and high-speed passenger rail development in North America. As part of a study funded by the Federal Railroad Administration (FRA) aimed at improving concrete crossties and fastening systems for US high speed rail and joint passenger/freight corridors, this research is aimed at developing a detailed 3D finite element (FE) model of a crosstie and fastener system using ABAQUS. The FE model consists of concrete crosstie and fastener system based on actual product design, and is loaded through practical static loading after prestress release. Nonlinear material property models as well as component tangential and vertical interactions are incorporated into the model. Comparison focused on different loading scenarios is carried out using the model to further look into the impact on the performance of the track system.

Keywords: Finite Element Method, Concrete Crosstie, Fastening System.

INTRODUCTION

With the development of high speed rail corridors and ever increasing axle loads in North America, there is an increasing demand on the railroad infrastructure and its components. Furthermore, the dominant design approach for the concrete crosstie and fastening system is mainly iterative. This is evident by the fact that the relation using speed and traffic to determine the design load in American Railroad Engineering and Maintenance-of-way Association (AREMA)'s Recommended Practices has been developed empirically¹. To ensure the safety of transportation and that proper track geometry is maintained, further investigation into the behavior and interaction of concrete crosstie and fastening system is needed. In addition, a mechanistic design approach based on detailed structural analysis would be beneficial for infrastructure manufacturers to reduce costs on overdesigned parts and efficiently improve future design work.

Researchers have done some innovative research in the modeling of the concrete crosstie and fastening system. Yu and Jeong² presented a 3D finite element model including prestressed concrete crosstie and ballast. Prestress and direct railseat loading is applied to look into its behavior. A quarter-symmetric model was used to compare the performance of the concrete crosstie on different support conditions. The model is limited since it assumes full bond between the concrete and strand, hence it ignores the possibility of relative slip of strands causing the effect of prestress to be magnified. Yu et al.³ presented an improved finite element model of the concrete crosstie with ballast and subgrade support. In this model the interaction between concrete and strand is modeled as cohesive element which is incorporated between them to simulate a linear force-slip relationship based on experiment data⁴. With the model built several factors that could affect the performance of the concrete crosstie are investigated including strand pattern and different ways to apply loading. As the modeling of concrete crosstie and fastening system is a broad topic, various researchers have used finite element analysis to gain a better understanding about its behavior and their research work provided some insight into the application of this technique^{5,6}.

Based on a thorough literature review some potential for improvement could be summarized and implemented in this research. As part of a large project funded by the Federal Railroad Administration (FRA), the objective of this research is to build a detailed 3D finite element model of the concrete crosstie and fastening system. The model will serve to provide theoretical comparison for ongoing laboratory and field testing as well as a tool to perform parametric studies of component material properties and geometric dimensions, which would be conducted to serve the general goal of developing new mechanistic design criteria for the concrete crosstie and fastening system to satisfy the ever-increasing loading demand in North America. In this paper a detailed 3D concrete crosstie and fastening system model is presented under various loading scenarios including prestress force, vertical wheel loading and lateral wheel loading at different levels. The finite element program ABAQUS was utilized in the study. Nonlinear material properties are defined for components based on manufacturer data. Frictional interaction is defined between different components. A study is conducted using the model on how different lateral/vertical loading ratio would affect the load path through fastening system and the stress state of the system.

MODELING CONFIGURATION

SYSTEM DESCRIPTION

The concrete cross tie is a structural element used on the track to support wheel loading and distribute loading over a larger area upon ballast. Fig. 1 illustrates the different components of a fastening system. As shown, the fastening system is fixed to concrete cross tie to transmit loading from rail to concrete surface and maintain uniform track geometry. Fastening systems of various designs are used in practice and different systems consist of different components. The fastening system modeled in this paper includes embedded iron shoulder, clip, nylon insulator, and a two part rail pad assembly consisting of resilient polyurethane 95 Shore, a pad for load attenuation and a nylon 6/6 abrasion plate to mitigate abrasion of the concrete. The embedded shoulder provides support for other components. The clip is deformed initially and inserted into shoulder to prevent longitudinal and lateral displacement of the rail. The insulator is placed between the clip and rail to provide electrical isolation between the two rails to ensure the signal system is not shunted. In working environment the wheel loading can be divided into a vertical loading, which is applied on the head of rail and a lateral loading that is pointing from gage side to the field side. In this model the geometry of all the components is simplified to reduce calculation time.

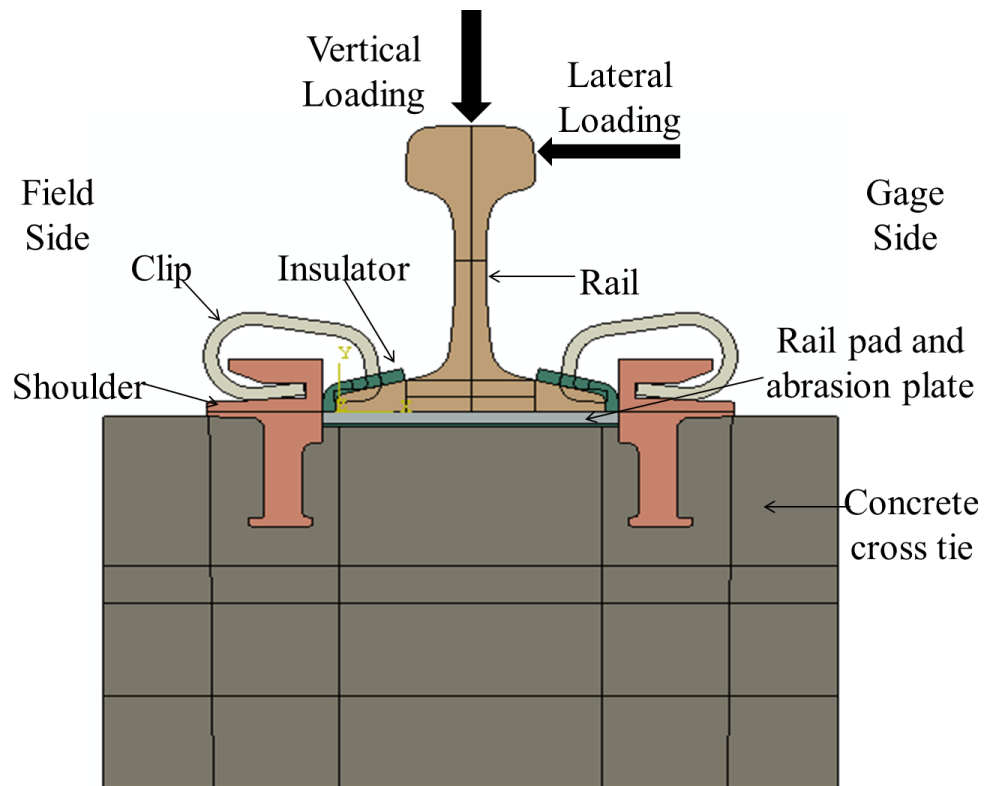


Fig. 1 Example layout of rail fastening system

CONSTITUTIVE RELATIONSHIPS

Concrete damaged plasticity model is used to define the concrete material property⁷. This model is suitable for cases where concrete is subjected to monotonic, cyclic or dynamic loading when confining pressure is relatively low. In this material model, two main failure mechanisms are considered, namely, tensile cracking and compressive crushing. As shown in Fig. 2, under uniaxial tension concrete first goes through a linear-elastic stage, and when stress reaches cracking stress it follows a softening stress-strain relationship. Under uniaxial compression the initial response is linear until the yielding stress is reached. In the plastic stage the response is first characterized by strain hardening and then strain softening after reaching its compressive ultimate stress. As cyclic loading is not included in the current model, two damage parameters related to unloading stiffness are not defined. Important material property parameters are listed in Table 1. 3D solid element with first order accuracy is used to define concrete element.

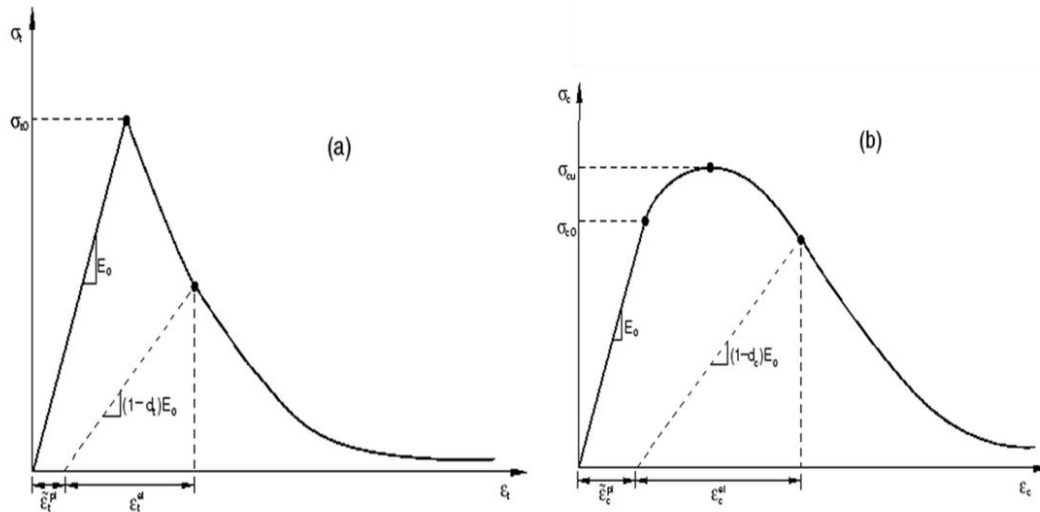


Fig. 2 Concrete stress-strain relationship under (a) uniaxial tension and (b) uniaxial compression

Table. 1 Material property data of model components

Component	Young's Modulus (psi)	Poisson's Ratio	Yielding Strength (psi)	Ultimate/Peak Strength (psi)	Cracking Strength (psi)
Concrete	4346640	0.2	NA	7000	800
Clip	23000000	0.29	183000	202060	
Rail	30000000	0.3	150000	150000	
Insulator	440000	0.39	9300	12300	
Rail Pad	7500	0.49	1200	5200	
Abrasion Plate	440000	0.39	9300	12300	

For all the fastening system components including shoulder, clip, rail pad, abrasion plate, insulator as well as the rail, a two-stage material property model is defined. In the beginning it follows an elastic relationship, and the plastic stage consists of a strain-hardening range followed by a strain-softening range. Important parameters are also included in Table. 1. These components are modeled with 3D solid element.

PRELIMINARY MODEL OF PRESTRESSED CONCRETE CROSSTIE

Prior to modeling the fastening system, a full-scale concrete crosstie model is built to investigate concrete prestress distribution after release. The model is built based on the design of CXT-505S crosstie. Concrete material property used in this model is the same as described above. Twenty straight prestressed strands are included in this model and are modeled as truss elements. Connector element is used to define the interaction between concrete and prestressed strand. Concrete is meshed in a way that element nodes along the line of strand coincide with strand node and a connector element will connect a coincident concrete node and a strand node. Acting as a spring, the connector will only restrain relative displacement along the direction of strand.

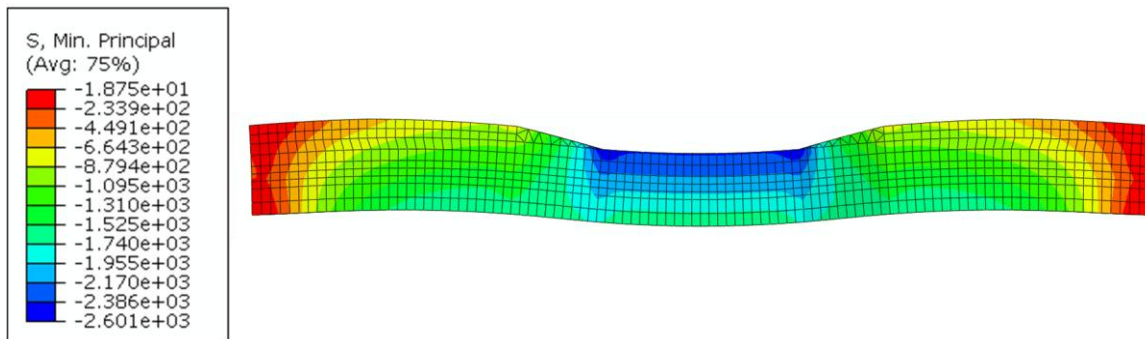


Fig. 3 Minimum principal stress contour of concrete crosstie after prestress release

Fig. 3 shows the minimum principal stress contour of concrete crosstie after release. As shown in the figure concrete crosstie is in a combination of compression and bending. A total prestress force of 140 kips is applied to concrete crosstie, and as the resultant force is not applied at the centroid of the section and the section changes throughout the length of concrete crosstie, different bending direction is observed at midspan and at the two ends. This model provides estimation for the prestress to be applied on the more detailed fastening system model as discussed later.

COMPONENT INTERACTION

Interaction between different fastening system components is defined with contact pairs in ABAQUS.⁷ A master surface and a slave surface of different mesh densities are identified. For tangential interaction between different components, the coefficient of friction (CoF) is assumed to be 0.3. This value was based on a series of large-scale abrasion resistance tests

that were conducted recently at the University of Illinois at Urbana-Champaign (UIUC) but not published yet.

To focus on the interaction between concrete and fastening system, the concrete crosstie is simplified into a concrete block that is close to the support of fastening system. Prestressed strands are not modeled and the effect of concrete prestress is applied through pressure on the lateral surface.

The interaction between the concrete block and shoulder inserts is difficult to simulate as it is related to multiple surface and could have tensile stress between the two components. In this model the cohesive stress between concrete and shoulder inserts are ignored. Slots according to the geometry of shoulder inserts are cut in concrete and interaction pairs are defined between the internal surfaces of concrete and the surface of shoulder inserts, which means that only compressive interaction is considered in the model.

Based on manufacturer design, in this model the insulator and the shoulder were modeled with a gap of 0.15 inch in between. This is important because the interaction between the shoulder and insulator considerably affects the load path through the fastening system under lateral loading. Due to this gap, lateral resistance first comes from the friction between the abrasion plate and concrete and the uneven clamping force due to rail sliding. As the insulator and shoulder come in contact, the resistance from the shoulder will share part of the loading.

BOUNDARY CONDITION AND LOADING

Boundary condition is applied at the bottom of concrete. Roller support is defined on the surface so that vertical displacement is restrained but lateral displacement and rotation are allowed. In the center of this surface fixed boundary condition is applied on a band of 6 inches to provide lateral resistance for the system.

Multiple analysis steps are defined to apply different types of loading. In the first step, prestress is applied on concrete by applying a pressure of 900 psi on the lateral surface. The value is determined after reviewing the effective prestress around shoulder in the full-scale concrete crosstie model which was described earlier. In the second step, pressure loading is applied on the toe surface of clips to simulate the process of clip lifting. On each clip, a load of 3500 lb is applied to exert excessive deformation prior to releasing the clip toe in following step. The pressure loading increases linearly with time. In the third step, the pressure on the toe of insulator gradually decreases with time as the clips are slowly released on to the insulator to apply the design clamping force. At the same time a temporary pressure loading of 100 psi is applied on the top surface of insulator to stabilize the system and is removed at the end of this step. In the fourth step, a vertical load of 30 kips is introduced on the rail head, and in the fifth step, a lateral load is introduced according to the loading scenario. The loading is designed according to the loading environment expected to be encountered in North American low-speed (speed lower than 40 miles per hour) mainline freight segment. The distribution of loading between concrete crossties at a spacing of 19 in

is assumed and the ratios between vertical and lateral loading considered in this model are 0.25 and 0.5¹. Both of the loads are introduced as pressure over a small area to simulate the contact patch in practice.

RESULTS

The analysis includes five steps in total and in each step, different loading is applied. As mentioned earlier, the first three steps are used to simulate the service condition for concrete crosstie and fastening system by applying prestress on the concrete crosstie and clamping force on the rail. Based on output after the release of clip, a clamping force of about 3000 lb is applied on each side of the rail.

In working condition the wheel of a vehicle would apply both a vertical load and a lateral load to the rail through the contact patch on the top and lateral surface of rail head. On curved track usually the loading condition is determined by the ratio between vertical and lateral load (L/V ratio). In this model two L/V ratios of 0.25 and 0.5 were considered. After prestress and clamping force are applied, a vertical load of 30 kips is applied on the top of rail head as pressure loading over an area of 1 in². The loading transfers from rail to rail pad, abrasion plate, and finally to the concrete. The compression of different components in the center of loading area is compared. The majority of vertical compressive deformation came from that of rail and concrete as a result of material property and geometry. The rail and concrete makes up of the majority of model thickness and would in turn allow for more compression deformation. While rail is much stiffer than concrete in compression, the section of rail is much smaller than concrete and therefore would result in high compressive stress at rail web. In addition, the compression deformation of rail pad is larger than that of abrasion plate as the material for rail pad (polyurethane) is softer than that of abrasion plate (Nylon). As the rail is relatively stiff it distributes the compressive stress onto a small area in the center of rail pad. Under vertical loading the dominant behavior of rail pad and abrasion plate is due to Poisson's effect as they expand laterally. Friction resists the lateral movement between the rail pad and abrasion plate as well as between abrasion plate and concrete-leading to an almost circular distribution.

STRESS ANALYSIS

Table 2 shows the maximum tensile and compressive stresses of different components in different loading scenarios (L/V ratio=0.25 and 0.5). In the loading scenario with lower lateral loading (L/V ratio=0.25), maximum compressive stress in concrete was recorded close to the extension of shoulder insert as the clip is pulling the shoulder out of concrete as shown in Figure 4. However, it is still below the compressive strength of concrete (i.e. 7000 psi). Maximum tensile stress occurred under the bottom of shoulder insert and was less than the concrete cracked strength. Clip steel starts to yield in tension right after releasing on to insulators, and under vertical and lateral loading it yields both in tension and compression on the interior and exterior surface, respectively. For insulator, maximum compressive stress is at the contact point with clip. Due to flexural effect, maximum tensile stress is observed at

the bottom surface of insulator. As rail pad is relatively soft, the maximum compressive stress is considerably higher than the yielding stress but still lower than the ultimate strength. The behavior of abrasion plate is similar to rail pad but it is still in elastic range. Maximum compressive and tensile stresses in the rail are located at the web due to flexure.

Table. 2 Maximum stress comparisons for different components in two loading scenarios

Component	Maximum compressive Stress (psi)		Yielding Strength or f_c' (psi)	Maximum Tensile Stress (psi)		Yielding or cracking Strength (psi)
	L/V = 0.25	L/V = 0.5		L/V = 0.25	L/V = 0.5	
	Concrete	6250		19944	7000	
Clip	197073	206029	183000	201877	223064	183000
Insulator	12288	20364	9300	4811	13360	9300
Rail Pad	4834	6449	1200	225	1100	1200
Abrasion Plate	4435	5954	9300	371	1414	9300
Rail	27166	44056	150000	14669	32479	150000

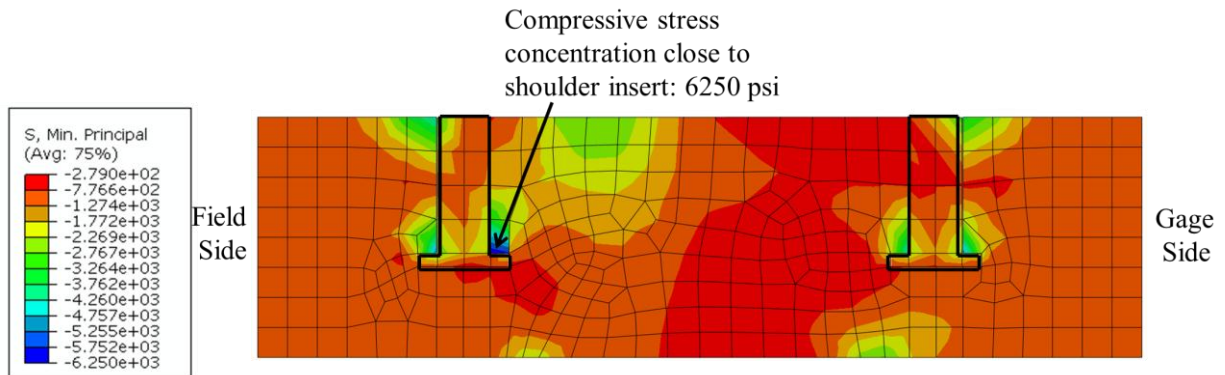


Fig. 4 Concrete section compressive stress contour (L/V ratio=0.25)

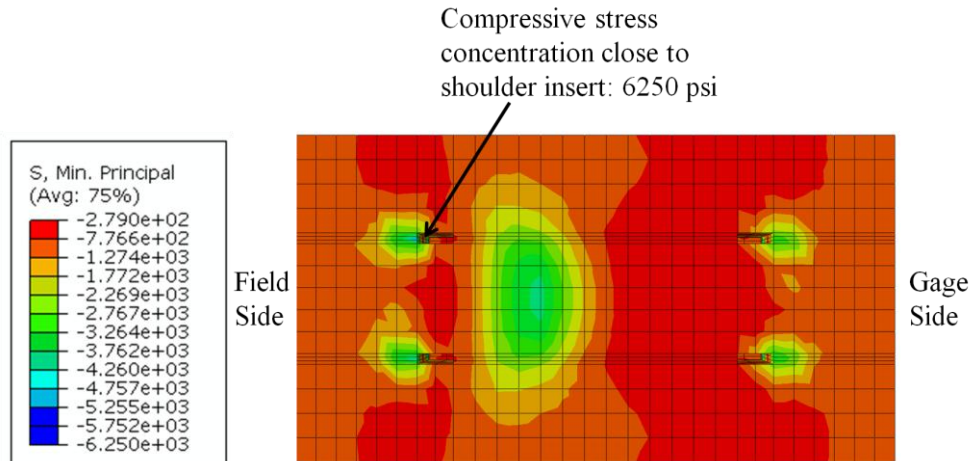


Fig. 5 Concrete surface compressive stress contour (L/V ratio=0.25)

As shown in Fig. 5, the compression zone due to vertical loading shifts to the field side. In addition, as the clamping force on the two sides is different due to lateral loading, the reaction force on shoulder is also different. In Fig. 4 it is shown that the compressive stress concentration around shoulder insert is more severe on field side than on the gage side, at the same time the vertical compressive stress due to rail head loading is inclined to the field side. The area surrounded by dark line is the position of shoulder insert.

When lateral load increases to 15 kips (i.e. L/V ratio=0.5), as shown in Fig. 6 and Fig. 7, the compressive stress concentration of concrete is at the top surface of concrete due to the compression of shoulder insert. As the shoulder is in contact with the insulator, a large portion of lateral loading is transferred from the rail to the shoulder through the insulator and results in local stress concentration in shoulder support. Based on the compressive stress value the concrete is already crushed. High tensile stress is recorded around shoulder insert slot and results in concrete cracking.

The stress distribution of the clips, the rail pad and the abrasion plate under higher lateral loading is similar to what described above with a L/V ratio of 0.25, but the maximum compressive and tensile stress increased due to larger deformations. For the insulator on the field side maximum compressive stress is found on the lateral surface that is in contact with the shoulder and the maximum tensile stress is found on the parallel surface which is in contact with the rail. The material has yielded both in tension and compression.

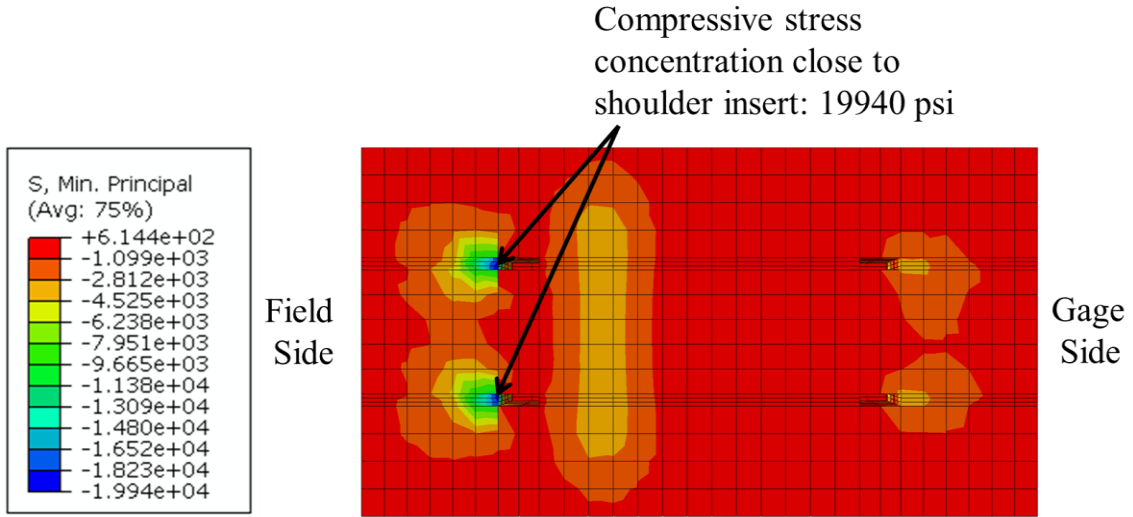


Fig. 6 Concrete surface compressive stress contour (L/V ratio=0.5)

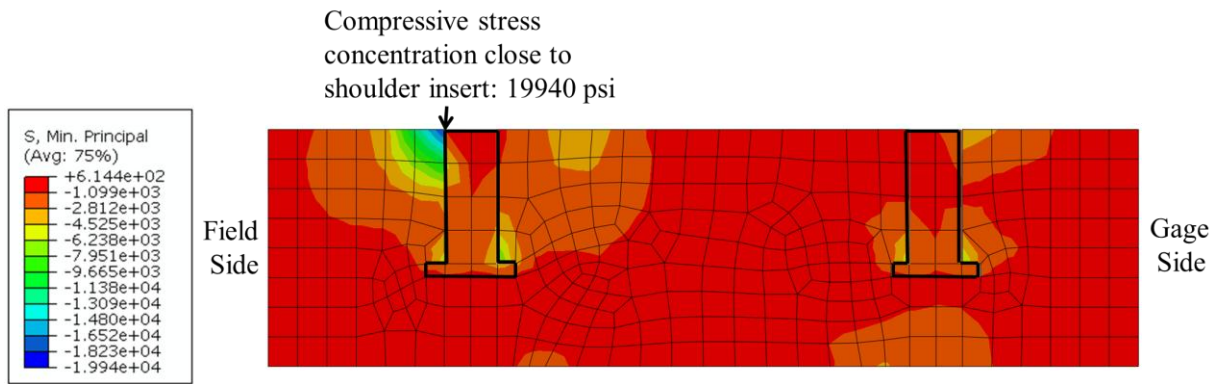


Fig. 7 Concrete section compressive stress contour (L/V ratio=0.5)

DEFLECTION ANALYSIS

The lateral resistance of rail consists of several parts: the friction between rail and rail pad, the lateral component of clamping force and the support force transferred through the insulator when the lateral displacement of rail is large enough to close the gap between insulator and shoulder. The displacement of rail head under vertical and lateral loading is an important criterion as it determines the support condition of the wheel. The displacement of rail under vertical and lateral loading is a combination of translation and rotation: clamping force from clips acts as the resistance for rotation and friction between rail and rail pad acts as the resistance for translation. Under a lateral loading of 7.5 kips the majority of lateral resistance came from rail seat friction (6.6 kips). At this point there is still a gap between insulator and shoulder therefore supporting force from shoulder should be zero. Based on model output it is shown that rail translation is the dominant mode and clip on the gage side

would be further released while the toe displacement of field-side clip increased by a small amount.

In the loading scenario with L/V ratio of 0.5, the lateral load increases linearly with time to the magnitude of 15 kips. When the lateral load reaches 10 kips, due to rail translation, the insulator will come in contact with the shoulder and the lateral supporting force would be applied on rail through the insulator. Afterwards rotation becomes the dominant displacement mode of the rail as shoulder prevents it from further translation. As a result in this stage the clamping force on the gage side is the major resistance for rail displacement, and the clip on the field side has little effect on restraining the rotation of rail.

Fig. 8 shows the relationship between lateral load and rail head lateral displacement. For track alignment Federal Railroad Administration (FRA) Track Safety Compliance Manual⁸ requires that on curved track of class 5 track the deviation of the mid-ordinate from a 31-foot chord may not be more than 0.5 in. Under a lateral loading of 7.5 kips (L/V ratio = 0.25) the lateral displacement of rail head is still within the acceptable range. However as lateral loading increased to 15 kips (L/V=0.5), the insulator got in contact with shoulder and the rail head lateral displacement increased to 0.8 in. It is also required that the base of rail does not move laterally more than 0.5 in relative to the cross-tie, and as shown in Fig. 9, the lateral translational displacement of rail is only 0.22 in due to the support of shoulder.

In this model the lateral bending stiffness of rail is ignored as the support condition on the ends of a rail segment is not simulated. In addition, the existence of gap between insulator and shoulder on the field side significantly affect the lateral resistance of rail. In practice the gap on the field side is usually closed after a few loading cycles and shoulder would prevent any further lateral displacement of the rail. For these limitations the lateral displacement of rail is overestimated in this model.

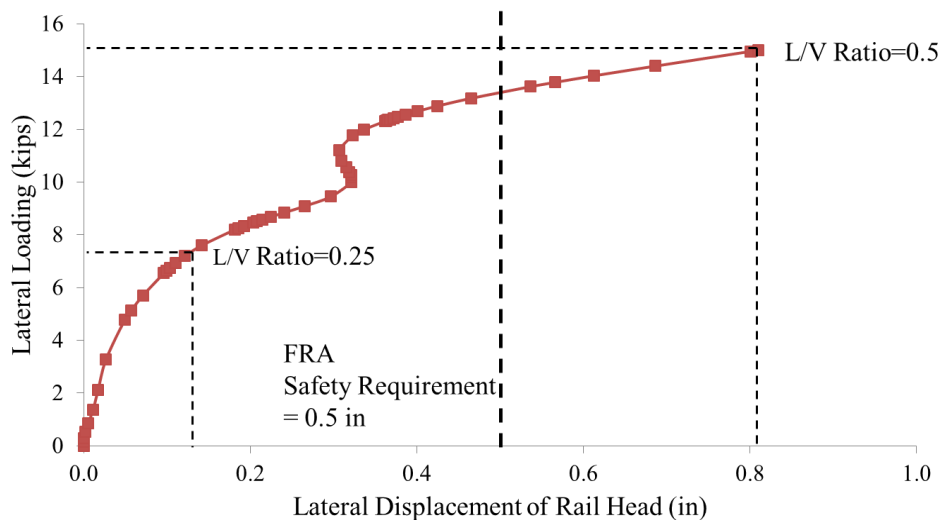


Fig. 8 Relationship between lateral loading and the lateral displacement of rail head

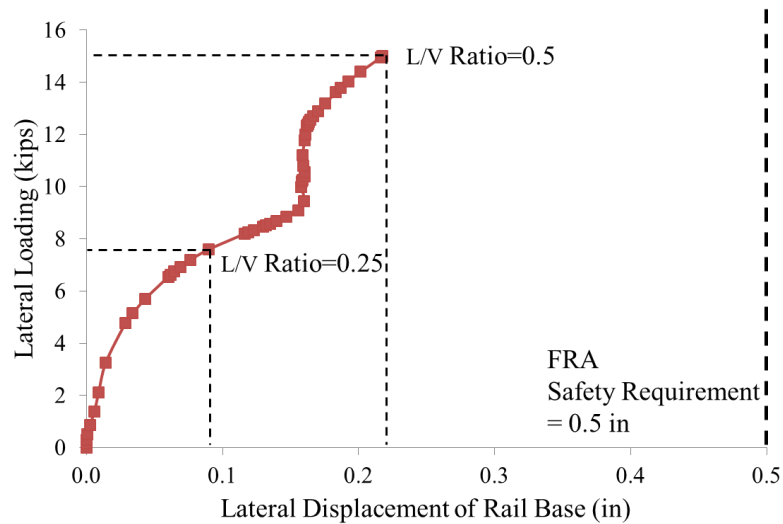


Fig. 9 Relationship between lateral loading and the lateral displacement of rail base

CONCLUSIONS

In this paper a detailed 3D finite element model for a crosstie and fastening system is presented. The FE model consists of concrete crosstie and fastening system based on actual product design, and is loaded through practical static loading after prestress release. Nonlinear material property models as well as component tangential and vertical interactions are incorporated into the model. Two different loading scenarios (L/V ratio=0.25 and 0.5) are considered and some conclusions are summarized:

- Due to material property and geometry under vertical loading the vertical deformation is mainly due to the compression of rail and concrete. The compression of rail pad is much larger than that of abrasion plate.
- When L/V ratio equals to 0.25, translation is the dominant displacement mode of rail, and when insulator start to come in contact with shoulder due to increasing lateral loading (10 kips) the dominant displacement of rail change to rotation.
- When L/V ratio equals 0.25, concrete stress concentration is observed close to the extension of shoulder insert, but the crushing or cracking stress limit are not researched. When L/V ratio equals 0.5 severe stress concentration exceeding the crushing and cracking strength of concrete is observed around shoulder inserts in concrete surface on the field side.

- Both the lateral displacement of rail base and rail head are within the track safety requirement under a lateral loading of 7.5 kips (L/V ratio=0.25). However when the lateral loading increased to 15 kips (L/V=0.5), the lateral displacement of rail base remain within the acceptable range for the support of shoulder, but the lateral displacement of rail head increased to 0.8 in and exceeded the safety requirement.

ACKNOWLEDGEMENT

The published material in this paper represents the position of the authors and not necessarily that of DOT. The authors would like to express sincere gratitude to Federal Railroad Administration for providing funding for this project. In addition, the authors also want to thank Jose Mediavilla (Amsted Rail), Pelle Duong (CXT Concrete Ties), and the following FRA Crosstie and Fastener BAA Industry Partners for providing product information and advices for research work:

- Amsted RPS / Amsted Rail, Inc.
- BNSF Railway
- CXT Concrete Ties, Inc., LB Foster Company
- GIC Ingeniería y Construcción
- Hanson Professional Services, Inc.
- National Railway Passenger Corporation (Amtrak)
- Union Pacific Railroad

The authors also would like to specially thank Riley Edwards, Marcus Dersch, Professor Daniel Kuchma, Professor Erol Tutumluer and Professor David Lange for their invaluable insight and experience. This work would not be possible without the contribution from Christopher Rapp, Brandon Van Dyk, Ryan Kernes, Sihang Wei, Justin Grasse, and Amogh Shurpali.

REFERENCE

1. American Railway Engineering and Maintenance-of-way Association (AREMA), "AREMA manual Chapter 30 Ties". 2009.
2. Yu, H., and Jeong, D.Y., 2010. "Finite Element Modeling of Railroad Concrete Crosstie – A Preliminary Study". International Conference of Railway Engineering, Beijing, China.
3. Yu, H., Jeong, D., Choros, J. and Sussmann, T., "Finite Element Modeling of Prestressed Concrete Crossties with Ballast and Subgrade Support," *Proceedings of the ASME 2011 International Design Engineering Technical Conference &*

- Computers and Information in Engineering Conference*, DETC2011-47452. August 2011, Washington, DC, USA.
4. Abrishami, H. and Mitchell, D., "Bond characteristics of pretensioned strand," *ACI Materials Journal*, Vol. 90, No. 3, May-Jun. 1993, pp. 228-235.
 5. Lundqvist, A. and Dahlberg, T., "Load Impact on Railway Track due to Unsupported sleepers," *Proc. IMechE Part F: J. Rail and Rapid Transit*, Vol. 219, Part. F, 2005, p. 67-77.
 6. Kaewunruen, S. and Remannikov, A. M., "Investigation of Free Vibrations of voided Concrete Sleepers in Railway Track System," *Proc. IMechE Part F: J. Rail and Rapid Transit*, Vol. 221, 2007, p.495-507.
 7. Dassault Systèmes Simulia Corp. "ABAQUS Analysis User's Manual."
 8. Federal Railroad Administration. "Track Safety Standards Compliance Manual: Chapter 5 Track Safety Standards Classes 1 through 5."2006.